



Field observations of sand flux and dust emission above a gobi desert surface

Xuesong Wang^{1,2} · Chunlai Zhang¹

Received: 13 October 2020 / Accepted: 18 January 2021 / Published online: 24 February 2021
© The Author(s), under exclusive licence to Springer-Verlag GmbH, DE part of Springer Nature 2021

Abstract

Purpose Gobi deserts are a major source of natural and anthropogenic aerosols in China. However, the characteristics of the sand flow and dust emission processes are still an open question. This study intends to accurately describe the characteristics of the sand flow and dust emission and to determine the relationship between the sand transport rate and the vertical dust flux above a gobi surface.

Materials and methods In this study, a field observation was conducted over a gobi (gravel) desert surface (Yangguan Gobi Desert, Gansu Province, China). We investigated the wind velocity, sand flux, and concentration of particles smaller than 10 μm (PM_{10}) by using cup anemometers, a sonic anemometer, sand traps, and DustTrak.

Results and discussion We found that (1) piecewise regression described the vertical sand flux profiles; the upper part of the profile (above 17 cm) should be described by a power function and the lower part should be described by a Gaussian function. (2) An empirical model based on the modified Owen equation could predict the sand transport rate accurately. (3) The vertical dust flux was described well by $F_v \propto u_*^3$ and the dust emission above the gobi surface should follow $A\rho u_* (u_*^2 - u_{*t}^2)$, where A is an empirical regression coefficient. (4) The efficiency of saltation bombardment (F_v/Q) was linearly related to the ratio u_{*t}/u_* .

Conclusions The results of this study show that the characteristics of the sand flow and dust emission above a gobi surface were highly different from those of bare sandy surface. In future research, it will be necessary to account for the effect of surface characteristics, and particularly the characteristics of the gravel, to improve the predictive ability of our model.

Keywords Sand transport rate · Dust emission · Gobi desert · Model · Vertical dust flux

1 Introduction

Gobi deserts, which have a gravel-dominated surface, are an important type of landform in arid regions of northwestern China, where they are widely distributed and cover an area of 661,000 km^2 (National Forestry Bureau 2011). Gobi deserts are mainly developed from the alluvial fans and are

characterized as “wide, shallow basins of which the smooth rocky bottom is filled with sand, silt or clay, pebbles or, more often, with gravel” (Cooke 1970; Owen et al. 1997; Vassallo et al. 2005). These deserts are a major source of natural and anthropogenic aerosols in China (Zhang et al. 2003; Wang et al. 2011), so it is important to observe and quantify dust emissions from their surfaces. Therefore, understanding eolian sand transport and dust emission processes in these deserts has both theoretical and practical importance. Currently, as for eolian sand transport and dust emission processes, most focuses have been paid on the sandy surface. However, they are different from that over gobi surfaces because of the presence of gravels or cobbles (Gillies et al. 2007). Compared with sandy surfaces, fewer attempts have been made to describe the blown sand and dust flux profiles over gobi surfaces (Dong et al. 2004). This, as a result, cause many difficulties for people assessing eolian processes on rough surfaces.

It is crucial to reliably predict vertical profiles of eolian sand flux because this information is necessary to estimate

Responsible editor: Yi Jun Xu

✉ Chunlai Zhang
clzhang@bnu.edu.cn

¹ State Key Laboratory of Earth Surface Processes and Resource Ecology, MOE Engineering Research Center of Desertification and Blown-sand Control, Faculty of Geographical Science, Beijing Normal University, No. 19 Xijiekouwai Street, Beijing 100875, China

² School of Environment, Beijing Normal University, No. 19 Xijiekouwai Street, Beijing 100875, China

sand transport rates, validate computer models, and understand the modified sand–wind flow and the vertical intensity of eolian abrasion. Since Bagnold (1941) and Chepil (1945) made their first attempts to measure the vertical mass flux profile, and discovered that it decreases rapidly with increasing height, significant progress has been made based on experimental studies conducted in wind tunnels, field observations, numerical simulations, and theoretical analyses (Ni et al. 2003). However, results have differed among studies (Ni et al. 2003). In addition, most of these studies investigated eolian sand flux above sandy surfaces; and fewer have investigated that above gobi surface (Dong et al. 2004; Qu et al. 2005; Tan et al. 2014). Thus, details of the transport behavior above the gravel surface of a gobi desert remain unclear. As a result, field observations of eolian sand flux above gobi surfaces are essential.

A central issue in studying eolian sand transport is how to predict the rate of sediment transport by the wind. Researchers have developed many models to predict sediment transport rates using the free-stream wind speed (U) or shear velocity (u_*). Based on a summary of representative published models by Dong et al. (2003), these models can be divided into five basic types: the Bagnold type, the modified Bagnold type, the O'Brien–Rindlaub type (O'Brien and Rindlaub 1936), the modified O'Brien–Rindlaub type, and the complex type. The O'Brien–Rindlaub type and the modified O'Brien–Rindlaub type are easy to apply, but they use wind velocity at a given height and they cannot account for the physical mechanisms that underlie wind erosion. The complex models, which are usually produced through numerical simulations, generally contain several parameters that are difficult to quantify. To avoid these problems, we restricted the present analysis to Bagnold-type models and modified Bagnold-type models of sand transport above a gobi surface. However, these models also present many drawbacks. First, published models are based at least partially on a set of assumed ideal conditions (Davidson-Arnott et al. 2008; Ellis and Sherman 2013), which greatly limits their application in the field. The disagreements between predicted and observed transport rates can largely be attributed to the fact that environmental factors (e.g., fetch length, slope, soil moisture content, and gravel content) in natural settings differ from the idealized assumptions used by the models (Sherman et al. 1998, Sherman et al. 2013; Barchyn et al. 2014). Furthermore, these models rely on saturated sand flux conditions, which occur infrequently in the field. Thus, it is essential to use field data to evaluate and calibrate these models.

Also, we designed the present study to provide some of the missing knowledge, and focused on two main aspects of gobi deserts. First, we studied the relationship between the shear velocity and the vertical dust flux above a gobi surface. Nickling and Gillies (1989, 1993) noted that the relationship between the shear velocity and the vertical dust flux differed

widely among study sites with different soil textures, vegetation cover, land use, anthropogenic disturbance, and other characteristics. Second, we examined which kind of model was most suitable for predicting dust emission above a gobi surface. There are three main types of dust emission model: empirical forms, energy-based forms, and forms based on volume removal by the wind (Gillette and Passi 1988; Shao et al. 1993; Marticorena and Bergametti 1995; Kok et al. 2012). In this study, it was important to select an appropriate dust emission model that was capable of accurately predicting the dust emission from a gobi desert.

Our overall goal was to accurately describe the characteristics of the sand flow and dust emission above a gobi surface. Our specific goals were (1) to describe the vertical profiles of eolian sand flux and find the most suitable model type for a gobi surface; (2) to quantify the relationship between the shear velocity and the vertical dust flux and use this knowledge to identify the most suitable dust emission scheme for gobi surface; and (3) to clarify the relationship between the sand transport rate and the vertical dust flux.

2 Methods

2.1 Field site

The study site is located in Yangguan, Gansu Province, northwestern China (40.13° N, 94.03° E). The study site is a wide, open, and flat mountain pass in the Yangguan Gobi Desert (Fig. 1). The surface mainly consists of gravel ranging from 20 to 150 mm in diameter. Gravel covers from 30 to 40% of the surface, and there is no vegetation. Fine sand is the main size class that underlies the gravel (with a mean grain size of 145 μm). Detailed information of the grain size distribution (< 2 mm) is described in Fig. 2. The study area has a typical continental hyper-arid climate with an average annual rainfall of 63 mm. Easterly and westerly winds prevail in the area and are strongest in April, when they are strong enough to transport sediment.

2.2 Data collection

We installed a sand trap, nine cup anemometers, a sonic anemometer, and three DustTrak (TSI Inc., Shoreview, MN, USA) aerosol monitors at the field site (Fig. 3).

The sand trap used to measure the sand flux was constructed from 10 sand collection chambers (each 100 mm deep \times 20 mm wide \times 10 mm tall), a steel frame with a removable cover, and a rectangular steel box at the bottom with a removable cover. The sand chambers were mounted behind the openings (20 \times 20 mm) whose lower edges were positioned at 0, 3, 7, 11, 16, 22, 29, 38, 48, and 58 cm above the surface. The sand trap was deployed perpendicular to the dominant

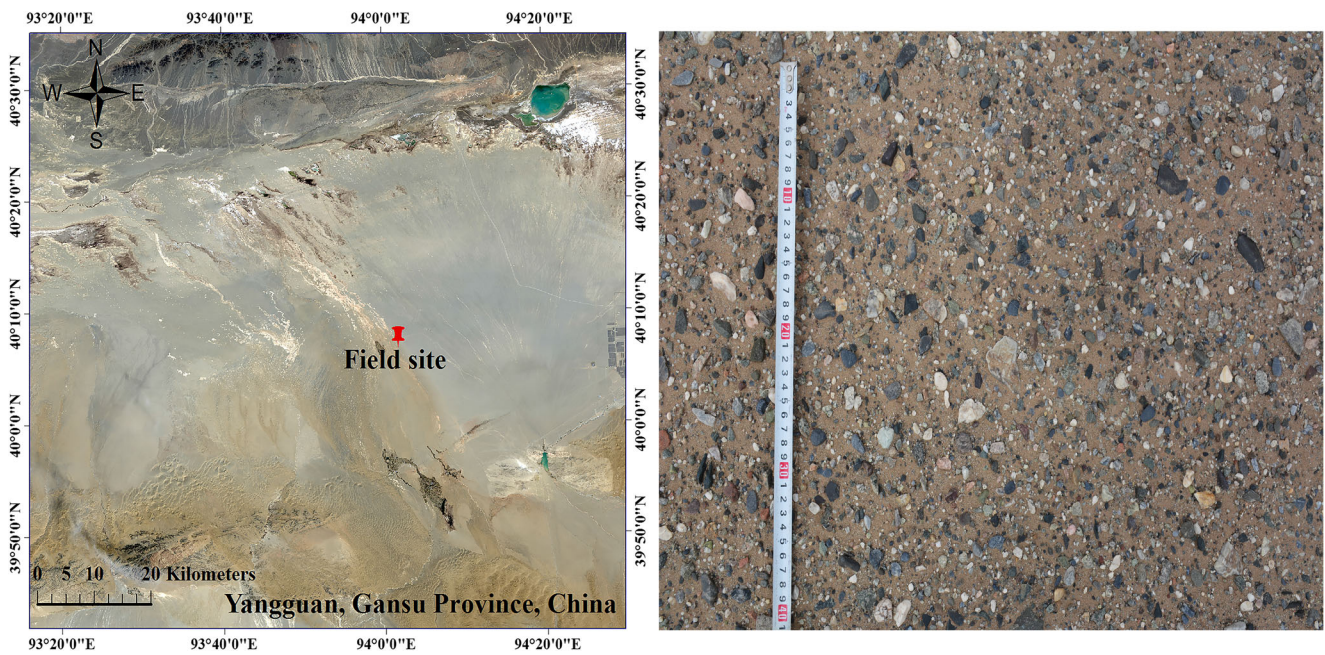


Fig. 1 The location of the field study site and photograph of the studied surface. Source: <http://www.gscloud.cn/>

sand-transporting wind direction and the openings were aligned parallel to the prevailing wind direction. Because the sand transport rate is closely related to the wind velocity, the duration of each sampling period was determined by the wind velocity. That is, to make the collected sand samples sufficiently large for analysis, we designed short sampling periods when wind velocities were high and long sampling periods when wind velocities were low. The specific sampling periods are described in the next section.

Profiles of the wind velocity at elevation z above the surface (U_z) were measured using the nine cup anemometers (which were calibrated to an accuracy of 0.1 m s^{-1} in a wind tunnel) at heights of 5, 10, 20, 30, 50, 75, 100, 200, and

300 cm. Wind velocity was recorded at 30-s intervals using a data logger; thus, the results represented average wind speeds, rather than instantaneous ones. At the same time, a sonic anemometer (model 81000; R.M. Young Co., Traverse City, MI, USA) was deployed, with an acquisition frequency of 32 Hz, to obtain high-frequency, three-dimensional wind vector data at a height of 100 cm. The three instruments were arranged side by side, but separated by 300 cm to prevent mutual interference. These instruments measured sediment entrainment, wind profiles, and the three-dimensional wind vectors concurrently.

Suspended dust was measured using DustTrak (TSI Inc.) aerosol monitors mounted at heights of 5, 60, and 200 cm. PM_{10} concentrations were sampled at 5-s intervals and averaged over a 1-min period so that they could be synchronized with the wind velocity measurements. We only observed one severe dust storm during our field study, on 1 May 2017; on that date, we only measured the suspended dust from 17:09:00 to 18:09:00.

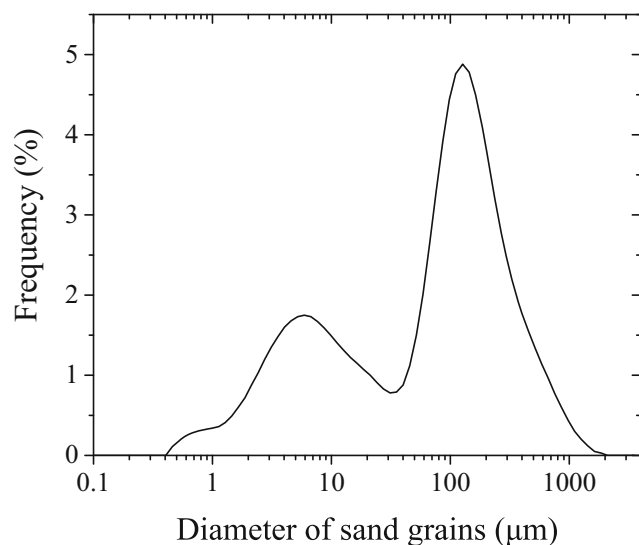


Fig. 2 Particle grain size distribution of the sand (<2 mm)

2.3 Data analysis

2.3.1 Shear velocity (u_* and u_{*RS})

We determined u_* using the equation $u_* = mk$, where m is the slope of the logarithmic function of the wind profiles which are determined by means of least squares curve fitting, and k represents Karman’s constant (0.4). This method was used by Dong et al. (2001) and Zhang et al. (2014).

The shear velocity derived from the Reynolds stress (u_{*RS}) values was obtained as follows:

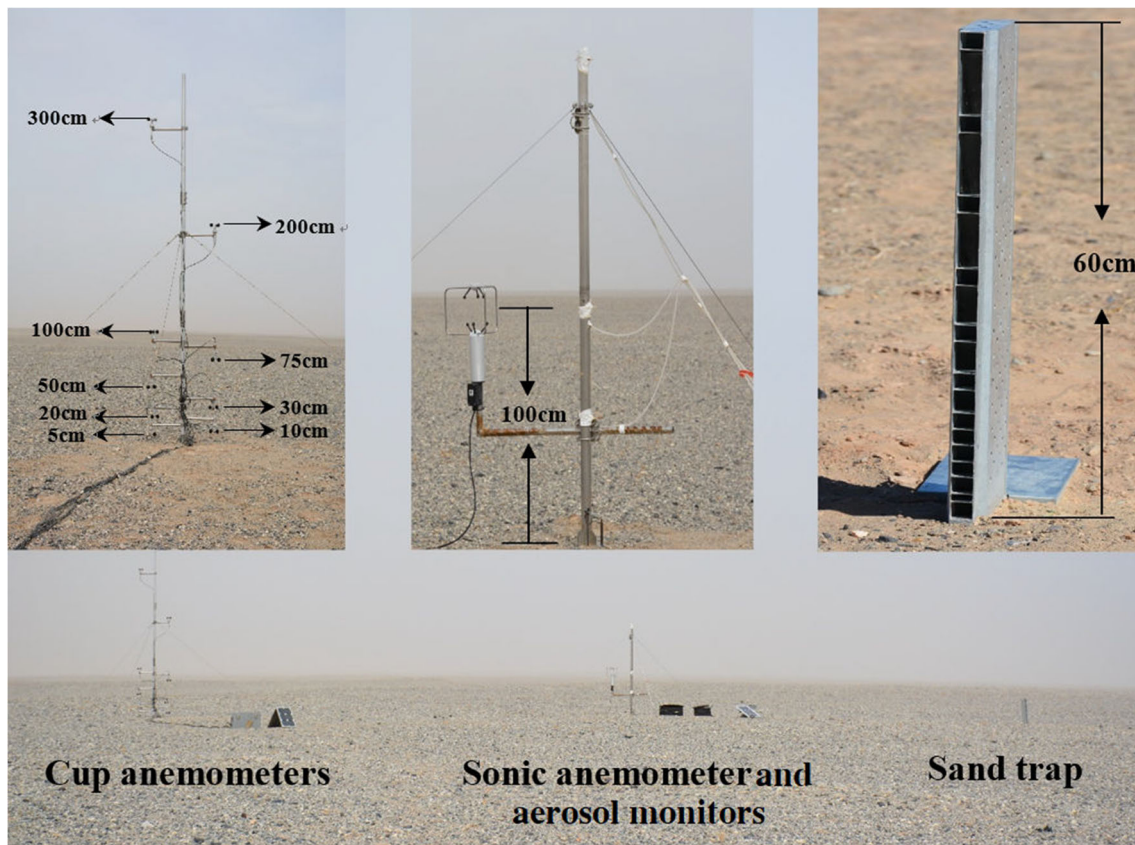


Fig. 3 Illustration of the instruments and their layout at the gobi surface study site

According to Reynolds (1995), the three wind vector components can be decomposed into mean (u, v, w) and fluctuation (u', v', w') components:

$$\begin{aligned} u &= \bar{u} + u' \\ v &= \bar{v} + v' \\ w &= \bar{w} + w' \end{aligned} \quad (1)$$

Although turbulent flow is a three-dimensional problem, the u and w components are thought to be the most important. Thus, the Reynolds stress (RS) can be calculated using the following equation:

$$RS = -\rho u' w' \quad (2)$$

where ρ is the density of air (1.25 kg m^{-3}) and $u' w'$ is the covariance between the u component and the w component of the wind vector.

Then, based on the relationship between shear stress (τ) and u_* ($\tau = \rho u_*^2$), the Reynolds stress turbulence parameter u_{*RS} can be calculated as follows:

$$u_{*RS} = \sqrt{|u' w'|} \quad (3)$$

Both RS and u_{*RS} can be measured directly using a sonic anemometer, in contrast to the mathematical calculation used for the profile-derived u_* .

2.3.2 Sediment transport

Referencing the method of Nickling and Gillies (1989, 1993), the sand flux transport rate (Q , $\text{kg m}^{-1} \text{ s}^{-1}$) can be estimated using the following equation given that the majority of the sediment transport above a gobi surface occurs within 200 cm above the surface (Wu 1987):

$$Q = \int_0^{200} q(h) dh \quad (4)$$

where $q(h)$ is the horizontal sand flux density ($\text{kg m}^{-2} \text{ s}^{-1}$) at height h above the surface. The specific function of $q(h)$ will be discussed in Section 3.1.2.

2.3.3 Coefficient of variation of the wind for different runs

The mean free-stream wind velocity (U) during an erosion period (an erosion period equals which from opening the sand trap to collecting the sand samples) can only be used to obtain u_* if the wind speed is stable or varies only slightly; thus, it is necessary to calculate the coefficient of variation (CV) of the

wind speed for each period. CV is defined as the ratio of the standard deviation (σ) to the mean (μ).

Following the system suggested by Wilding (1985), in which samples are considered to be highly variable when $CV > 0.35$, moderately variable when $0.35 > CV > 0.15$, and slightly variable when $CV < 0.15$, we can conclude that the wind was stable for each of the 36 erosion periods ($CV < 0.15$) (Table 1), and that using U to derive u_* is reasonable.

2.3.4 The PM₁₀ vertical flux

We calculated the vertical flux ($F_{v,5-200}$, mg m⁻² s⁻¹) of PM₁₀, which represents suspended dust, according to the gradient method of Gillette and Walker (1997), using the following equation:

$$F_v = \frac{u_*k(C_5 - C_{200})}{\ln\left(\frac{z_{200}}{z_5}\right)} \tag{5}$$

where C_5 and C_{200} are the concentrations (mg m⁻³) of PM₁₀ at heights of 5 and 200 cm, respectively, and z_5 and z_{200} are the height of the bottom and top of the region covered by the DustTrak device, respectively.

3 Results

3.1 Sand flow observations

3.1.1 Vertical profiles of eolian sand flux

Above a sandy surface, the amount of sediment transported by saltation generally decreases rapidly with increasing height. However, different functions have been proposed to model this trend. The most commonly cited function is exponential (Dong et al. 2003), but other studies have also produced successful models using a power form (Zingg 1953) or a logarithmic form (Rasmussen and Mikkelsen 1998). We found that the vertical distribution of sand flux at a height of 60 cm above the gobi surface differed from that above a sandy surface; it showed a peak flux at a certain height above the surface, after which the flux decreased rapidly (Fig. 4a). This phenomenon, described as an “elephant trunk” by Qu et al. (2005), because of the shape of the curve, has also been reported in other studies (Dong et al. 2004; Tan et al. 2014). Dong et al. (2004) reported that sand flux profiles could be expressed by Gaussian distribution functions. We found that the profile above a gobi surface could only be described by a Gaussian distribution ($R^2 > 0.94$ for all periods) below a height of 17 cm (Fig. 4b). Above this height, the sand flux decreased with increasing height following a power function

Table 1 Summary of the data used in this study. CV, coefficient of variation; u_* , shear velocity; u_{*RS} , Reynolds shear velocity. Wind directions are measured clockwise from north (0°)

Period	Duration (min)	CV	u_* (m s ⁻¹)	u_{*RS} (m s ⁻¹)	Wind direction (°)	Period	Duration (min)	CV	u_* (m s ⁻¹)	u_{*RS} (m s ⁻¹)	Wind direction (°)
1	30	0.080	0.426	0.559	261.8	19	1	0.011	0.583	0.791	272.5
2	30	0.072	0.431	0.547	261.2	20	1	0.020	0.800	0.897	272.9
3	30	0.092	0.408	0.522	265.8	21	1	0.051	0.772	0.877	268.9
4	30	0.093	0.407	0.507	267.4	22	1	0.077	0.593	0.784	267.8
5	30	0.121	0.375	0.521	264.4	23	1	0.080	0.621	0.785	277.2
6	30	0.106	0.382	0.552	265.3	24	1	0.072	0.764	0.714	276.2
7	30	0.121	0.387	0.502	268.5	25	6	0.092	0.429	0.473	282.5
8	30	0.137	0.412	0.566	259.8	26	7	0.093	0.504	0.564	295.7
9	30	0.135	0.391	0.541	261.8	27	7	0.121	0.473	0.545	295.7
10	30	0.102	0.424	0.530	256.7	28	6	0.106	0.437	0.562	283.7
11	30	0.087	0.401	0.524	256.7	29	4	0.121	0.529	0.603	286.2
12	30	0.121	0.464	0.634	256.5	30	4	0.137	0.515	0.548	297.1
13	10	0.039	0.582	0.708	265.3	31	10	0.135	0.424	0.519	290.9
14	5	0.080	0.727	0.808	276.8	32	11	0.102	0.384	0.479	287.2
15	5	0.073	0.641	0.856	276.9	33	3	0.087	0.493	0.639	299.0
16	6	0.142	0.760	0.836	273.1	34	4	0.121	0.499	0.690	291.9
17	1	0.047	0.787	0.859	276.2	35	5	0.039	0.488	0.621	286.3
18	1	0.043	0.732	0.763	264.0	36	15	0.080	0.466	0.660	295.3

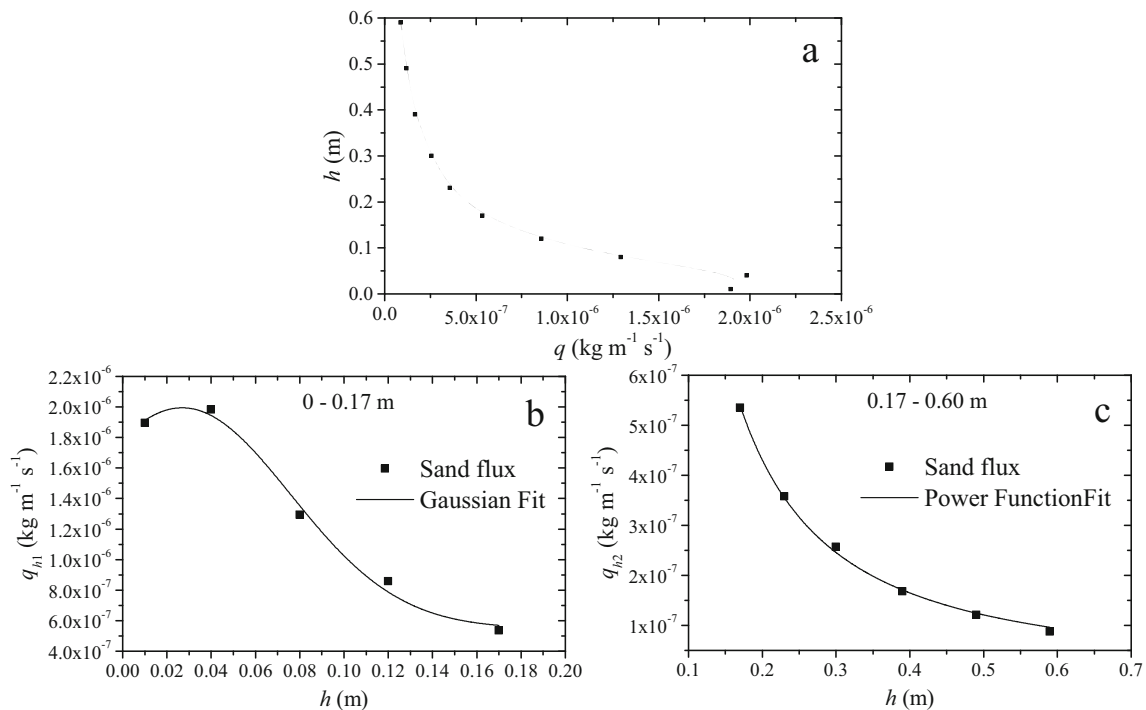


Fig. 4 Plots of the vertical distribution of sand flux for a representative example of the 36 erosion periods. **a** The vertical distribution of sand flux (q) as a function of height (h) above the gobi surface. **b** The relationship

between q_{h1} and h below 17 cm above the gobi surface, which follows a Gaussian function. **c** The relationship between q_{h2} and h above 17 cm above the gobi surface, which follows a power function

($R^2 > 0.92$ for all periods) (Fig. 4c). Based on these results, it appears that the vertical flux profiles above the gobi surface follow different forms of equations for different heights:

$$\begin{cases} q_{h1} = y_0 + A \exp\left(-0.5 \left(\frac{h-c}{w}\right)^2\right) & 0 \leq h \leq 0.17 \text{ m} \\ q_{h2} = a h^{-b} & h \geq 0.17 \text{ m} \end{cases} \quad (6)$$

where q_{h1} and q_{h2} are the sand flux density (in $\text{kg m}^{-2} \text{s}^{-1}$) at height h (m) below and above (respectively) the threshold height (17 cm) at which the equation form changes, and y_0 , A , c , w , a , and b are regression coefficients. It is noteworthy that the regression coefficient c characterizes the peak flux height, and the fitting results of Eq. (6) showed that the height of peak flux was slightly variable ($\text{CV} = 0.14$; Wilding 1985). By integrating Eq. (4), we found that the maximum flux density occurs at 3.4 cm above the gobi surface. Although we did not study this extreme point (the maximum flux density) further, we hypothesize that it is closely related to the size and coverage of the surface gravels. This hypothesis should be tested in future research.

3.1.2 Sediment transport model

Most sediment transport models, whether empirical or theoretical, are composed of three components (Gillette and Ono 2008): soil, airflow, and wind shear properties. Soil properties can be described by a dimensionless soil-related parameter

(A). For example, in the model by Dong et al. (2003), $A = f(d) = 1.41 + 4.98 \exp(-0.5(\ln(d/1.55D)/0.57)^2)$. Airflow properties are usually described using ρ/g (where ρ represents the density of air and g represents the acceleration due to gravity, 1.25 kg m^{-3} and 9.81 m s^{-2} respectively). Wind shear properties, which are potentially the most important part of the model, are usually described using $f(u_*)$ or $f(u_*, u_{*t})$. In this paper, we divide the eight models we studied to identify the optimal form into Bagnold ($Q = A(\rho/g)u_*^3$) and modified Owen ($Q = A(\rho/g)u_*(u_*^2 - u_{*t}^2)$) categories. Thereby, the models of Bagnold (1941), Zingg (1953), and Hsu (1971) belong to the Bagnold type and the models of Kawamura (1951), Owen (1964), Lettau and Lettau (1978), and Dong et al. (2003) belong to the modified Owen type.

To identify the most suitable model type, we calculated Pearson’s correlation coefficient (r) for the relationships between the measured transport rate and the wind shear properties (u_*^3 and $u_* [u_*^2 - u_{*t}^2]$, u_{*RS}^3 and $u_{*RS} [u_{*RS}^2 - u_{*t}^2]$), and we assumed that both soil and airflow properties did not change. We found that both model types had strong and statistically significant relationships with the measured transport rate. For $u_*^3 - Q$, $r = 0.91$, $p < 0.001$; for $u_* [u_*^2 - u_{*t}^2] - Q$, $r = 0.93$, $p < 0.001$; for $u_{*RS}^3 - Q$, $r = 0.85$, $p < 0.001$; and for $u_{*RS} [u_{*RS}^2 - u_{*t}^2] - Q$, $r = 0.88$, $p < 0.001$. However, the regressions based on the modified Owen models and based on u_* produced a better goodness of fit than the Bagnold-type models.

Thus, we concluded that the modified Owen model based on u_* ($Q = A(\rho/g)u_* [u_*^2 - u_{*t}^2]$) was the most suitable model for predicting sediment transport above a gobi surface. The dimensionless soil-related parameter A is the only unknown parameter in this model. Thus, we performed curve fitting to produce a functional form of the modified Owen-type model using version 8.0 of the Origin software (www.originlab.com/) to determine the value of A . Figure 5 shows significant strong or moderately strong relationships between the measured transport rate and both u_* and u_{*RS} . Again, u_* performed better than u_{*RS} , with a higher R^2 (0.88 versus 0.78). The estimated value of A was 2.01 based on u_* , so the sediment transport model for the gobi surface in this study therefore becomes $Q = 2.01 (\rho/g)u_* (u_*^2 - u_{*t}^2)$.

3.2 PM₁₀ emission

3.2.1 Temporal variability in PM₁₀ concentrations as a function of wind velocity

At about 17:09:00 on 1 May, obvious and continuous sand flow occurred in the study area, so we used the DustTrak aerosol monitors to measure the dust emission for 1 h. Figure 6a shows that, during the first 20 min, wind velocity fluctuated from 9.3 to 11.3 m s⁻¹. During this period, temporal variations of the PM₁₀ concentration at heights of 5, 60, and 200 cm above the surface showed a similar trend as a function of wind velocity (Fig. 6b–d). However, fluctuation of the PM₁₀ concentration was stronger at lower height than that at higher height. During the remaining 40 min, the wind velocity gradually increased. This trend was visible in the temporal variations of the PM₁₀ concentration at 5 cm. In contrast, the PM₁₀ concentrations at 60 and 200 cm did not increase gradually and continuously; instead, they increased first and then showed a decreasing trend. This means that the suspended dust was not thoroughly mixed with a uniform concentration near the surface in the atmospheric boundary layer during our observation. We analyzed the correlation between the PM₁₀

concentration and wind velocity by the Pearson correlation analysis, and we found that the PM₁₀ concentration at 5 cm was much more strongly correlated with the wind velocity ($r = 0.90, p < 0.001$) than the PM₁₀ concentrations at 60 cm ($r = 0.67, p < 0.001$) and 200 cm ($r = 0.75, p < 0.001$), which is consistent with the findings of Zobeck and van Pelt (2006). We therefore hypothesized that the emission and variations of PM₁₀ at 5 cm were mainly affected by the wind conditions, whereas the PM₁₀ concentrations at 60 and 200 cm are influenced by additional environmental factors like the suspended dust transported from upwind. The PM₁₀ concentrations measured at heights of 5, 60, and 200 cm are composed of dust emitted from the gobi surface and suspended dust transported from upwind. The PM₁₀ from non-local sources accounted for a larger proportion at the heights of 60 and 200 cm, and this weakened their correlations with wind velocity.

3.2.2 Dust vertical flux and shear velocity

Figure 7 shows the relationship between the PM₁₀ vertical flux (F_{v5-200}) and the shear velocity. The PM₁₀ vertical flux increased with increasing shear velocity following a power function. Nickling and Gillies (1989, 1993) used the relationship between PM₁₀ vertical flux and shear velocity to classify experimental sites based on their surface morphology and land use, and grouped the datasets accordingly. They found that the vertical flux is proportional to u_*^n , and that the value of n was determined by the surface morphology and land use. For undisturbed natural desert sites, $F_v \propto u_*^{2.99}$; for sites that developed from or were modified by fluvial processes, $F_v \propto u_*^{3.32}$; for construction sites, $F_v \propto u_*^{4.24}$; and for mine tailings, $F_v \propto u_*^{2.93}$. In the present study, Fig. 7 shows that, for the gobi surface, $F_v \propto u_*^{2.99}$, which is same as that for undisturbed natural desert sites in the previous research. It is now generally believed that the main mechanisms for dust emission are saltation bombardment and disaggregation (Shao 2008). Therefore, dust emission must be directly related to the intensity of saltation and indirectly related to wind shear at the

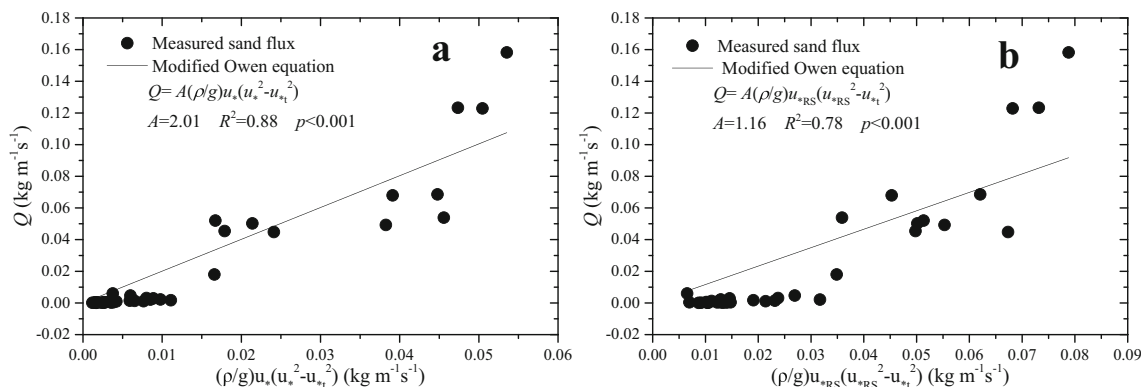


Fig. 5 Regression results for the relationship between the measured transport rate above the gobi surface ($Q, \text{kg m}^{-1} \text{s}^{-1}$) for **a** the shear velocity (u_*) and **b** the Reynolds shear velocity (u_{*RS}). Variables: A , regression coefficient; ρ , density of air; u_{*t} , threshold shear velocity

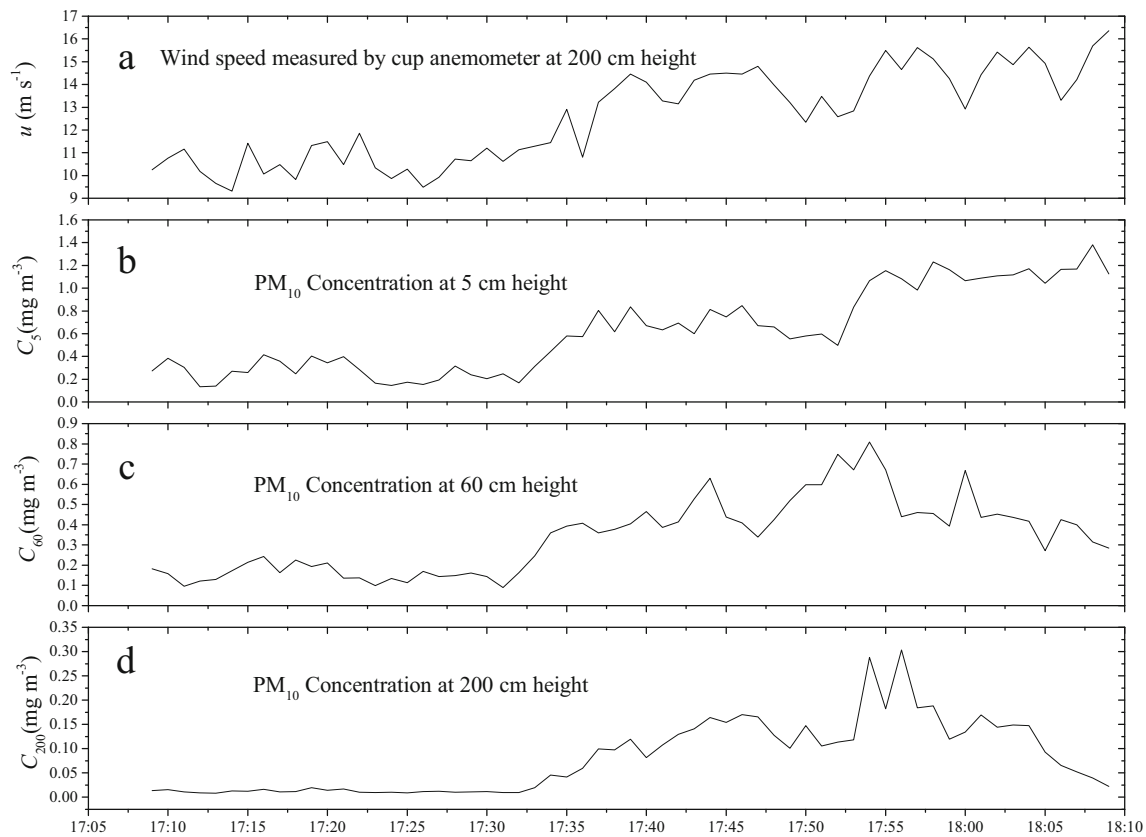


Fig. 6 Observation of the concentrations (C) of particles with diameters smaller than $10\ \mu\text{m}$ (PM_{10}) at heights of 5, 60, and 200 cm and their relationships with the free-stream wind velocity (u) at 200 cm during the

wind erosion period that was monitored between 17:09:00 and 18:09:00 on 1 May. (All values are 1-min means)

surface. Shao (2008) proposed that, for a hard soil, $F_v \propto u_*^3$, and for a soft soil, $F_v \propto u_*^4$. This is because saltation bombardment is less efficient in producing dust for a hard surface than for a soft surface. For the hard gobi surface we studied, saltation bombardment efficiency should be similar to that for a

hard soil because the dust particles were protected against saltating particles by the many gravel particles. Figure 7 supports this hypothesis; the exponent of 2.99 equals the exponent of 3 proposed by Shao.

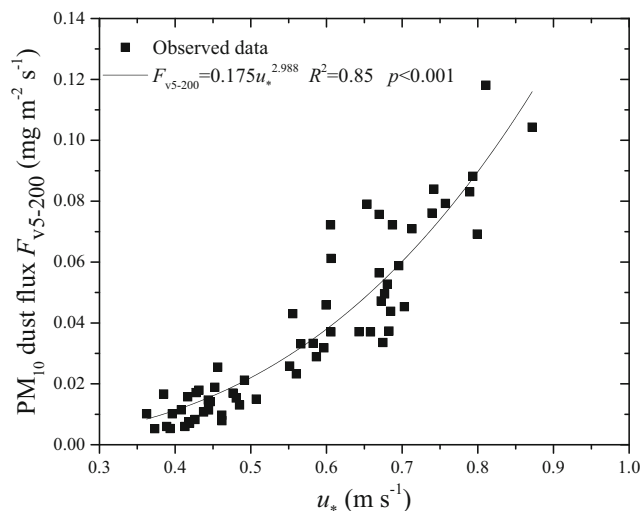


Fig. 7 Relationship between the vertical flux of particles smaller than $10\ \mu\text{m}$ in diameter (PM_{10}) between 5 and 200 cm ($F_{v,5-200}$) and the shear velocity (u_*)

3.2.3 Dust emission schemes

We used the data we obtained for the gobi surface to assess the prediction accuracy of four dust emission schemes (Gillette and Passi 1988; Shao et al. 1993; Marticorena and Bergametti 1995; Kok et al. 2012). Figure 8 shows that the model of Gillette and Passi (1988) performed worst among the four models ($R^2 = 0.67$). This is because their model suggested that the dust emission rate was proportional to u_*^4 , whereas our observed data suggested the dust emission rate was proportional to u_*^3 . The other three models performed better, but with similar R^2 values: 0.82, 0.84, and 0.85, respectively, for models of Shao et al. (1993), Marticorena and Bergametti (1995), and Kok et al. (2012). As Marticorena and Bergametti (1995) noted, the vertical dust flux should be proportional to the horizontal saltation flux because the saltation flux and the amount of kinetic energy it transfers to the soil surface have a similar scale to u_* . In the present study, the best saltation model was $A(\rho/g)u_* [u_*^2 - u_{*c}^2]$. This suggests that

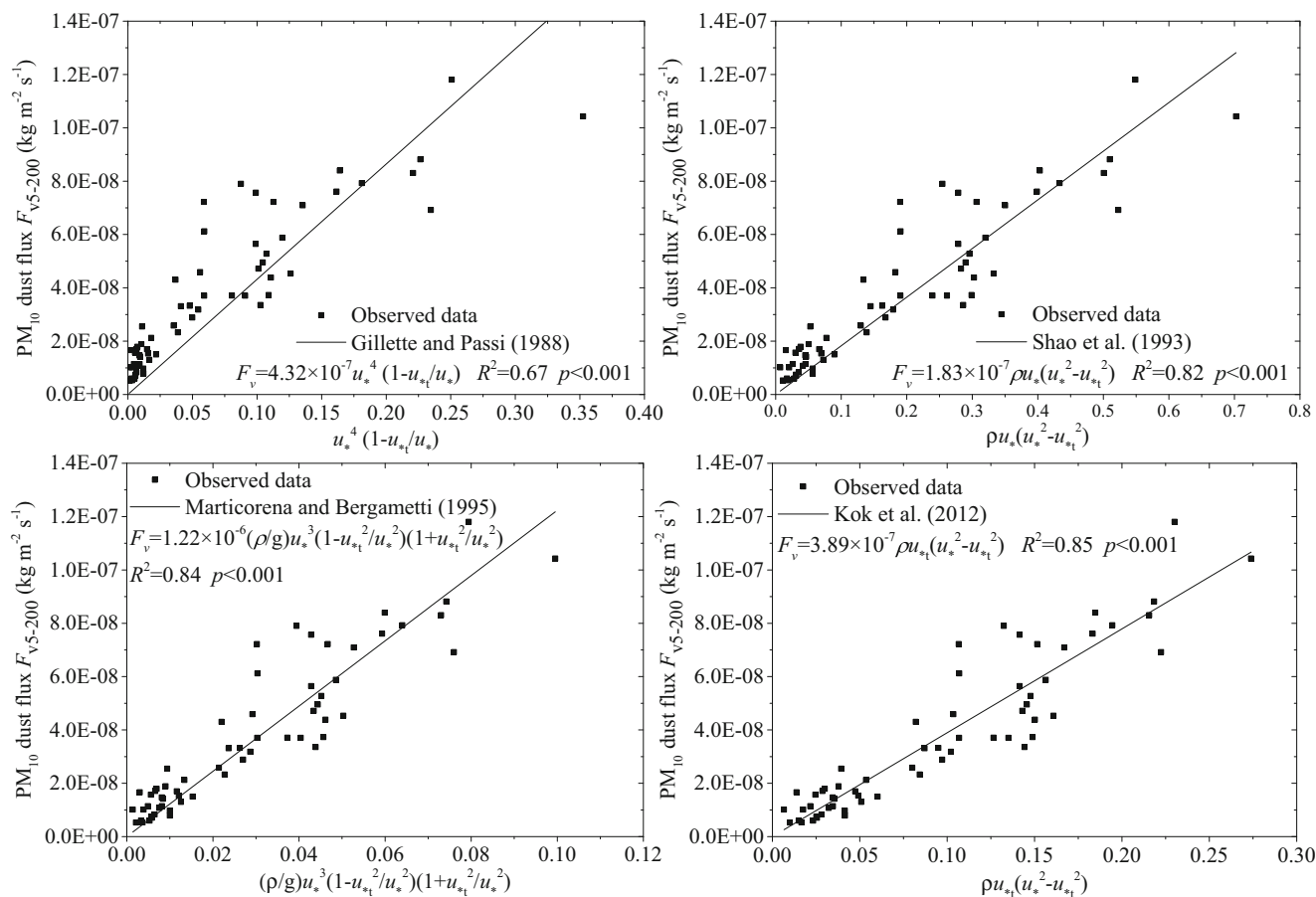


Fig. 8 Comparison of the vertical flux ($F_{v,5-200}$) of particles with a diameter smaller than $10\ \mu\text{m}$ (PM_{10}) predicted by four previous models

the dust emission model of Shao et al. (1993) should be the best choice. However, Kok et al. (2012) noted that the assumption that Shao et al. (1993) made about the speeds with which saltating particles impact the surface was incorrect. To be specific, the mean impact speed of saltating particles is independent of u_* for transport limited saltation. Kok et al. (2012) proposed a more reasonable model. Our results suggest that the model of Kok et al. (2012) was most suitable for predicting the PM_{10} vertical flux above a gobi surface. Thus, the dust emission scheme for a gobi surface should follow $A\rho u_{*t}(u_*^2 - u_{*t}^2)$. The values of parameter A (kg J^{-1}) should then depend on the surface conditions, including the gravel cover and grain size characteristics.

3.3 The efficiency of saltation bombardment

Shao et al. (1993) stated that, in a wind tunnel study of surface with no saltating particles introduced, there was little dust emission even at the maximum flow speed generated by the wind tunnel (about $20\ \text{m s}^{-1}$); in contrast, strong dust emission occurred if sand particles were propelled over the dust surface. They clearly

showed that F_v is proportional to Q and that saltation bombardment is a major mechanism responsible for dust emission. Thus, it is necessary to discuss the efficiency of saltation bombardment, which is described by the ratio F_v/Q (m^{-1}). Using the equation we developed for predicting the sand transport rate ($Q = 2.01 (\rho/g)u_* [u_*^2 - u_{*t}^2]$) and the equation for the vertical flux of dust ($F_v = 3.89 \times 10^{-7} \rho u_{*t} [u_*^2 - u_{*t}^2]$), we can further deduce that:

$$\frac{F_v}{Q} = 1.93 \times 10^{-7} \frac{u_{*t}}{u_*} \tag{7}$$

We can therefore conclude that the efficiency of saltation bombardment is linearly related to the u_{*t}/u_* ratio. Hence, for a surface whose threshold shear velocity is constant, the efficiency of saltation bombardment will decrease with increasing shear velocity. That is, although both the vertical flux of dust and the sand transport rate increase with increasing wind velocity, the rate of increase for the vertical flux of dust is lower than that for the sand transport rate. Additional research will be required to explain this difference.

4 Discussion

4.1 Difference between u_* and u_{*RS}

Compared to the sonic anemometer measurements, the data measured by the cup anemometers showed a stronger correlation with the sand transport rate. This may be due to the height at which the instruments were installed. That is, in our study, the sonic anemometer was installed at 100 cm above the surface and can therefore only measure wind at this point in the flow field. Owing to the relatively long distance, the effect of surface gravel on the airflow cannot be captured by the sonic anemometer, although this device could be used if multiple sonic anemometers could be installed at a range of heights in future research. In contrast, the cup anemometers were fixed at a range of heights from 5 to 300 cm. This enabled them to measure more of the airflow near the surface.

4.2 Discrepancy among the vertical fluxes of dust at different heights

Rajot et al. (2003) noted that estimates of vertical dust flux are often obtained by measuring dust concentrations at two heights and then applying a diffusion equation similar to Eq. (5) to interpolate between those heights. Currently, no standard heights have been specified for dust concentration measurements, and different researchers have therefore used different heights. The different heights would create a discrepancy in flux estimates unless the suspended dust is thoroughly mixed to achieve a uniform near-surface concentration in the atmospheric boundary layer. However, this assumption is not adequate for areas with actively eroding dust source regions, where large eroding surfaces contain heterogeneous areas with varying erodibility (Zobeck and van Pelt 2006). In the present paper, we calculated the dust vertical fluxes ($F_{v60-200}$) using the PM_{10} concentrations at 60 and 200 cm. Figure 9 shows a weak linear relationship between the vertical flux of dust and u_*^3 , with $R^2=0.24$ and $p<0.001$. However, as we noted earlier, vertical dust flux produced by the wind was described well by $F \propto u_*^3$ in our study area. We hypothesize that the dust concentrations we measured were not all produced by our measured wind. The correlations between the wind velocity and the dust concentrations at 5, 60, and 200 cm support this hypothesis. However, because the dust concentration produced by the wind increased with decreasing height (Kind 1992; Gillies and Berkofsky 2004), the dust concentration at a height of 5 cm produced by the measured wind was relatively high and was affected less by non-local dust. Thus, when we calculated the vertical flux of dust using the dust concentrations at 5 and 200 cm, the result was more reasonable and closer to the real value.

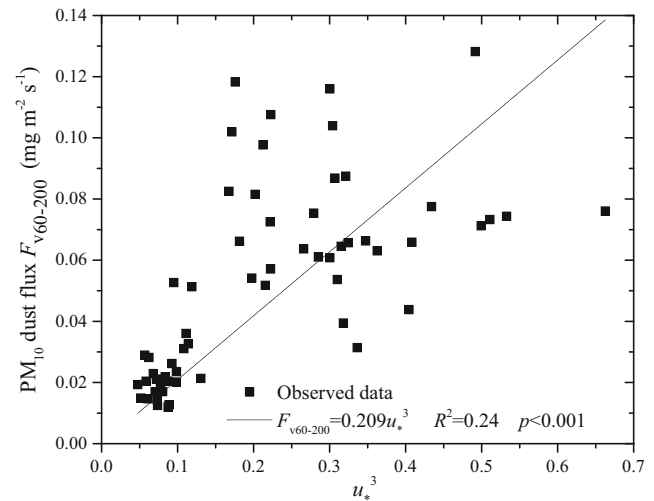


Fig. 9 Relationship between the vertical flux ($F_{v0.6-2}$) of particles smaller than $10 \mu\text{m}$ (PM_{10}) and the cube of the shear velocity (u_*^3)

5 Conclusions

In situ data of vertical sand flux and dust flux above the gobi desert surface have been studied in this study. It has demonstrated that the vertical profile of sand flux above a gobi surface is highly different from that above a sandy surface, and should be described by a Gaussian function (below 17 cm) and a power function (above 17 cm). By evaluating some classic sediment transport models, we found that the model $Q = A(\rho/g)u_*(u_*^2 - u_{*t}^2)$ is appropriate for predicting sand transport rate above a gobi surface. However, the values of parameter A depend on the surface characteristics like the gravel coverage, shape of the gravel, and gravel particle size distribution. Also, our observations suggest that dust emission scheme for a gobi surface follows the equation $F_v = A(\rho/g)u_{*t}(u_*^2 - u_{*t}^2)$, which means that the efficiency of saltation bombardment ($\frac{F_v}{Q}$) is linearly related to the u_{*t}/u_* ratio. This indicates that, for a surface whose threshold shear velocity is constant, the efficiency of saltation bombardment will decrease with increasing shear velocity.

Code availability Not applicable.

Author contribution Xuesong Wang did the experiments, analyze the data, and wrote the original manuscript. Chunlai Zhang designed the experiments and checked and revised the paper.

Funding This study was supported by the National Natural Science Foundation of China (No. 41630747).

Data availability Data will be available on request.

Declarations

Conflict of interest The authors declare no competing interests.

References

- Bagnold RA (1941) *The physics of blown sand and desert dunes*. Methuen, London
- Barchyn TE, Martin RL, Kok JK, Hugenholtz CH (2014) Fundamental mismatches between measurements and models in aeolian sediment transport prediction: the role of small-scale variability. *Aeolian Res* 15:245–251
- Chepil WS (1945) Dynamics of wind erosion: I. nature of movement of soil by wind. *Soil Sci* 60:305–320
- Cooke RU (1970) Stone pavement in deserts. *Ann Assoc Am Geogr* 60:560–577
- Davidson-Amott RGD, Yang Y, Ollerhead J, Hesp PA, Walker IJ (2008) The effects of surface moisture on aeolian sediment transport threshold and mass flux on a beach. *Earth Surf Process Landf* 33:55–74
- Dong Z, Gao S, Fryrear DW (2001) Drag coefficients, roughness length and zero-plane displacement height as disturbed by artificial standing vegetation. *J Arid Environ* 49:485–505
- Dong Z, Liu X, Wang H, Wang X (2003) Aeolian sand transport: a wind tunnel model. *Sediment Geol* 161:71–83
- Dong Z, Wang H, Liu X, Wang X (2004) A wind tunnel investigation of the influences of fetch length on the flux profile of a sand cloud blowing over a gravel surface. *Earth Surf Process Landf* 29:1613–1626
- Ellis JT, Sherman DJ (2013) *Fundamentals of aeolian sediment transport: wind-blown sand*. Treatise Geomorphol:85–108
- Gillette DA, Ono D (2008) Expressing sand supply limitation using a modified Owen saltation equation. *Earth Surf Process Landf* 33:1806–1813
- Gillette D, Walker TR (1997) Characteristics of airborne particles produced by winderosion of sandy soil, high plains of West Texas. *Soil Sci* 123:97–110
- Gillette DA, Passi R (1988) Modeling dust emission caused by wind erosion. *J Geophys Res* 93:14233
- Gillies JA, Berkofsky L (2004) Eolian suspension above the saltation layer, the concentration profile. *J Sediment Res* 74:176–183
- Gillies JA, Nickling WG, King J (2007) Shear stress partitioning in large patches of roughness in the atmospheric inertial sublayer. *Bound-Layer Meteorol* 122:367–396
- Hsu SA (1971) Wind stress criteria in eolian sand transport. *J Geophys Res* 76:8684–8686
- Kawamura R (1951) Study of sand movement by wind. *Hydraulics Engineering Laboratory Report HEL-2-8*. University of California, Berkeley
- Kind RJ (1992) One-dimensional aeolian suspension above beds of loose particles—a new concentration-profile equation. *Atmos Environ* 26:927–931
- Kok JF, Parteli EJR, Michaels TI, Karam DB (2012) The physics of wind-blown sand and dust. *Rep Prog Phys* 75:106901
- Lettau K, Lettau H (1978) Experimental and micrometeorological field studies of dune migration. In: Lettau HH, Lettau K (eds) *Exploring the world's driest climate*. Center for Climate Research, Univ. Wisconsin, Madison, pp 67–73
- Marticorena B, Bergametti G (1995) Modeling the atmospheric dust cycle: I. Design of a soil-derived emission scheme. *J Geophys Res* 100:15–30
- National Forestry Bureau (2011) *Bulletin of the states of desertification and aeolian desertification in China*, pp. 1–20
- Ni J, Li Z, Mendoza C (2003) Vertical profiles of aeolian sand mass flux. *Geomorphology* 49:205–218
- Nickling WG, Gillies JA (1989) Emission of fine-grained particulates from desert soils. In: Leinen M, Sarnthein M (eds) *Paleoclimatology and paleometeorology: modern and past patterns of global atmospheric transport*. Kluwer Academic, Dordrecht
- Nickling WG, Gillies JA (1993) Dust emission and transport in Mali, West Africa. *Sedimentology* 40:859–868
- O'Brien MP, Rindlaub BD (1936) The transportation of sand by wind. *J Comput Civ Eng* 6:325–327
- Owen PR (1964) Saltation of uniform grains in air. *J Fluid Mech* 20:225–242
- Qu J, Huang N, Quan T, Qiang L (2005) Structural characteristics of gobi sand-drift and its significance. *Adv Earth Sci* 20:19–23 In Chinese
- Owen LA, Windley BF, Cunningham WD, Badamgarav J, Dorjnamjaa D (1997) Quaternary alluvial fans in the Gobi of southern Mongolia: evidence for neotectonics and climate change. *J Quat Sci* 12:239–252
- Rajot JL, Alfaro SC, Gomes L, Gaudichet A (2003) Soil crusting on sandy soils and its influence on wind erosion. *Catena* 5:1–6
- Rasmussen KR, Mikkelsen HE (1998) On the efficiency of vertical array aeolian field traps. *Sedimentology* 45:789–800
- Reynolds O (1995) On the dynamical theory of incompressible viscous fluids and the determination of the criterion. *Philos Trans R Soc Lond A* 186:123–164
- Shao Y (2008) *Physics and modelling of wind erosion*, 2nd edn. Springer, New York
- Shao Y, Raupach MR, Findlater PA (1993) Effect of saltation bombardment on the entrainment of dust by wind. *J Geophys Res* 98:12719
- Sherman DJ, Jackson DWT, Namikas SL, Wang J (1998) Wind-blown sand on beaches: an evaluation of models. *Geomorphology* 22:113–133
- Sherman DJ, Li BL, Ellis JT, Farrell EJ, Maia LP, Granja H (2013) Recalibrating aeolian sand transport models. *Earth Surf Process Landf* 38:169–178
- Tan L, Zhang W, Qu J, Du J, Yin D, An Z (2014) Variation with height of aeolian mass flux density and grain size distribution over natural surface covered with coarse grains: a mobile wind tunnel study. *Aeolian Res* 15:345–352
- Vassallo R, Ritz JF, Braucher R, Carretier S (2005) Dating faulted alluvial fans with cosmogenic ^{10}Be in the Gurvan Bogd mountain range (Gobi-Altay, Mongolia): climatic and tectonic implications. *Terra Nova* 17:278–285
- Wang X, Zhang C, Wang H, Qian G, Luo W, Lu J, Wang L (2011) The significance of gobi desert surfaces for dust emissions in China: an experimental study. *Environ Earth Sci* 64:1039–1050
- Wilding LP (1985) Soil spatial variability: its documentation, accommodation and implication to soil survey. In: Nielsen DR, Bouma J (eds) *Soil spatial variability*. Proceedings of a workshop of the ISSS and the SSA, PUDOC, Wageningen, pp 166–187
- Wu Z (1987) *Geomorphology of wind-drift sands and their controlled engineering*. Science Press, Beijing (In Chinese)
- Zhang C, Zhou N, Zhang J (2014) Sand flux and wind profiles in the saltation layer above a rounded dune top. *Sci China Earth Sci* 57:523–533
- Zhang X, Gong S, Zhao T, Arimoto, R, Wang, Y, Zhou Z (2003) Sources of Asian dust and role of climate change versus desertification in Asian dust emission. *Geophys Res Lett* 30:2272
- Zingg A (1953) Wind tunnel studies of the movement of sedimentary material. In: *Proceedings of the 5th hydraulic conference*. State University of Iowa, Studies in Engineering Bulletin, 34:111–135
- Zobeck TM, Van Pelt RS (2006) Wind-induced dust generation and transport mechanics on a bare agricultural field. *J Hazard Mater* 132:26–38

Publisher's note Springer Nature remains neutral with regard to jurisdictional claims in published maps and institutional affiliations.